

# Volumetric abnormalities of the brain in a rat model of recurrent headache

Zhihua Jia<sup>1</sup>, Wenjing Tang<sup>1</sup>, Dengfa Zhao<sup>1</sup>, Guanqun Hu<sup>1</sup>, Ruisheng Li<sup>2</sup> and Shengyuan Yu<sup>1</sup>

Molecular Pain  
Volume 14: 1–11  
© The Author(s) 2018  
Reprints and permissions:  
sagepub.com/journalsPermissions.nav  
DOI: 10.1177/1744806918756466  
journals.sagepub.com/home/mpx



## Abstract

Voxel-based morphometry is used to detect structural brain changes in patients with migraine. However, the relevance of migraine and structural changes is not clear. This study investigated structural brain abnormalities based on voxel-based morphometry using a rat model of recurrent headache. The rat model was established by infusing an inflammatory soup through supradural catheters in conscious male rats. Rats were subgrouped according to the frequency and duration of the inflammatory soup infusion. Tactile sensory testing was conducted prior to infusion of the inflammatory soup or saline. The periorbital tactile thresholds in the high-frequency inflammatory soup stimulation group declined persistently from day 5. Increased white matter volume was observed in the rats three weeks after inflammatory soup stimulation, brainstem in the low-frequency inflammatory soup-infusion group and cortex in the high-frequency inflammatory soup-infusion group. After six weeks' stimulation, rats showed gray matter volume changes. The brain structural abnormalities recovered after the stimulation was stopped in the low-frequency inflammatory soup-infused rats and persisted even after the high-frequency inflammatory soup stimulus stopped. The changes of voxel-based morphometry in migraineurs may be the result of recurrent headache. Cognition, memory, and learning may play an important role in the chronification of migraines. Reducing migraine attacks has the promise of preventing chronicity of migraine.

## Keywords

Migraine, cutaneous allodynia, voxel-based morphometry, chronification

Date Received: 14 November 2017; revised 3 December 2017; accepted: 28 December 2017

## Introduction

Migraine is a primary headache disorder with high socioeconomic and personal effects.<sup>1</sup> Chronic migraine (CM) is the most common type of chronic daily headache seen by headache specialists.<sup>2</sup> Based on the current classification guidelines, CM is classified as a single entity, not a complication of migraine.<sup>3</sup> Migraine has been proposed to be a spectrum of illnesses, with clinical symptoms that vary in headache-day frequency and symptoms along a continuum from episodic migraine (EM) to CM.<sup>4</sup> Approximately 2.5% of patients with EM transform to CM annually.<sup>4</sup> With chronification, headache frequency increases and patients become more disabled and less responsive to therapy. Several risk factors have been associated with migraine progression, such as female sex, basic headache frequency, caffeine intake, and so forth.<sup>4</sup> However, the neurobiological

mechanisms by which some patients with EM progress to CM remain unclear.

As a noninvasive procedure, magnetic resonance morphometry has the potential to be the ideal tool for the quest to identify morphological substrates of the disease. One of the most widely used and validated morphometric techniques to capture structural alterations in the brain is voxel-based morphometry (VBM). VBM is a whole-brain method used to analyze automatically pre-processed structural high-resolution magnetic resonance

<sup>1</sup>Department of Neurology, Chinese PLA General Hospital, Beijing, China

<sup>2</sup>Research Center for Clinical and Translational Medicine, 302 Hospital of PLA, Beijing, China

### Corresponding Author:

Shengyuan Yu, Department of Neurology, Chinese PLA General Hospital, Beijing, China.

Email: yusy1963@126.com



imaging (MRI) data by treating images as continuous scalar measurements.<sup>5</sup> VBM has been used to investigate the pathophysiology of neuropsychiatric disorders, such as Parkinson's disease, Alzheimer's disease, essential tremor, and depression.<sup>6–8</sup> Several studies using VBM analysis have been performed in interictal migraineurs (mostly on patients with EM) and have reported that migraine has both decreases and increases gray matter volume (GMV) in pain transmitting and modulating areas.<sup>9–13</sup> Despite the important information obtained from imaging studies of migraineurs, the clinical relevance of this association is not clear. It is hard to control migraine attack completely on clinic, it is unknown whether the morphological changes reverse after migraine attacks stop.

Rats have a short life cycle and good homology, longitudinal brain imaging studies are much more feasible in rodent. Animal models of migraine are available and VBM studies have been performed in neuropathic pain and traumatic brain injury rodent models,<sup>14,15</sup> enabling investigations of brain structural changes in migraine animal models. The commonly used animal model of migraine involves repeated infusion of an inflammatory soup (IS) through a transcranial cannula to stimulate trigeminovascular and meningeal afferents.<sup>16</sup> The validity and reliability of this migraine model has been demonstrated in previous studies.<sup>17–19</sup> We prepared animal models to mimic EM and CM using different frequencies of IS administration. As a symptomatic manifestation of central sensitization, the majority of migraineurs develop cutaneous allodynia during migraine attacks and some have persistent sensitization even during the interictal phase.<sup>20,21</sup> Therefore, we also tested the time course of headache-induced cutaneous allodynia around the periorbital region of the rats. We chose the model described by Julie Wieseler because the polyurethane tubing was suitable for MRI scanning.<sup>19</sup> The primary aim of this study was to (i) investigate structural brain abnormalities in low frequency, high frequency, and extended high frequency of IS-stimulated groups, (ii) determine if the structural brain abnormalities reverse after IS stimulation is stopped, and (iii) try to reveal the possible neurobiological mechanisms related to cutaneous allodynia.

## Materials and methods

### *Ethical concerns and habituation*

Sixty specific-pathogen-free Sprague Dawley adult male rats (180–220 g; 6–7 weeks of age; Beijing Vital River Laboratory Animal Technology Co., Ltd.) were used. The rats were housed individually in a temperature-controlled ( $22 \pm 2^\circ\text{C}$ ) environment on a 12/12 h light/dark cycle with the lights turned on at 07:00 and allowed food and water ad libitum. The experimental procedures

were approved by the Laboratory Animal Center of the General Hospital of Chinese People's Liberation Army (Beijing, PR China) and were consistent with the ethical guidelines recommended by the International Association for the Study of Pain in experimental conscious animals.<sup>22</sup>

The rats were habituated for three days prior to the surgery. During the habituation period, the rats were placed in a plastic tube restraint and the researchers touched the periorbital region of its head several times with von Frey monofilaments (North Coast Medical Co., Ltd., Gilroy, CA, USA) to acclimate it to the testing apparatus, and then measured its baseline tactile sensory thresholds.

### *Groups*

The rats were divided randomly according to a sequence generated by a random-number table to avoid selection bias. According to the frequency and duration of IS infusion, the rats were assigned to five experimental groups and corresponding control (Con) groups ( $n = 6/\text{group}$ ), i.e., low-frequency infusion of IS (LF-IS; once every four days for three weeks); high-frequency infusion of IS (HF-IS; daily for three weeks); extended high-frequency infusion of IS (HF-IS-E; daily for six weeks); recovery after low-frequency infusion of IS (LF-IS-R; once every four days for three weeks, stopped for three weeks); and recovery after high-frequency infusion of IS (HF-IS-R; daily for three weeks, stopped for three weeks). The rats in the IS groups received infusions of IS (10  $\mu\text{L}$ ) for 5 min and the Con groups received sterile saline. The IS (2 mM histamine, 2 mM 5-hydroxytryptamine, 2 mM bradykinin, and 0.2 mM prostaglandin E2 in saline; Sigma, USA) was prepared from stock solutions prior to use. The mean duration of migraine was about 10 years in clinical studies and as pain is an unhappiness experience, three weeks in rats (approximate to 6–7 years in human) may be enough to mimic clinical attacks.<sup>23</sup> Rats infused with IS repeated three times per week for more than eight times developed a long-lasting decrease in periorbital pressure thresholds in previous study.<sup>24</sup> LF-IS group rats were infused with IS six times totally (less than eight times) to approximate the patients with EM. The HF-IS rats were infused with IS daily to mimic CM.<sup>24</sup> The animal group design is presented in Figure 1.

### *Surgical procedures*

The surgery was conducted according to the methods described in our previous research.<sup>17</sup> Briefly, the rats were placed under general anesthesia (pentobarbital 50 mg/kg, intraperitoneal) and positioned in a stereotaxic apparatus (ZS-B/C, Beijing, China). The duration of

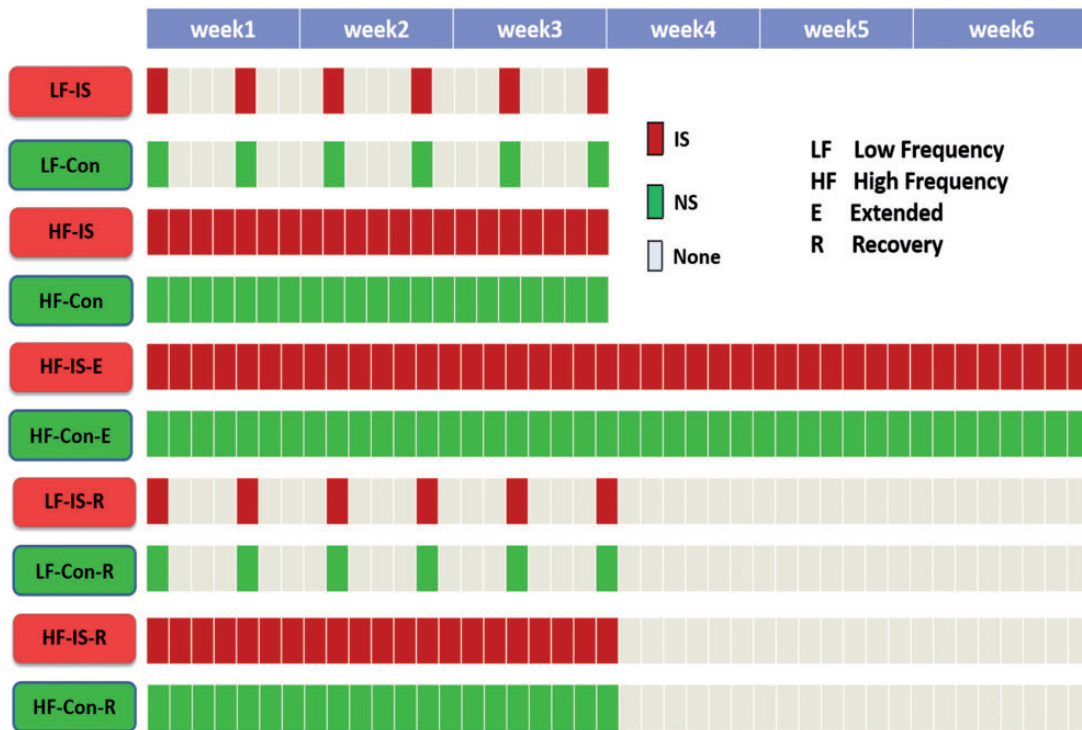


**Figure 1.** Experimental grouping. About one week after surgery, rats received the inflammatory soup (IS) or saline. The LF-IS group received IS once every three days for three weeks, the HF-IS group received the IS daily for three weeks, the HF-IS-E received the IS daily for six weeks, the LF-IS-R group received the IS once every four days for three weeks following three weeks of no infusion, and the HF-IS-R group received the IS daily for three weeks following three weeks of no infusion. Comparable control (Con) groups are indicated. IS: inflammatory soup; Con: control.

surgery was about 15 min. An incision was made on the scalp to expose the skull. Next, two 8- to 10-mm long, 2-mm wide and  $\sim 0.5$ -mm deep troughs bilateral to the midsagittal suture (3–4 mm lateral to it) were drilled in the skull to orient and secure the PE10 tubing (62310; RWD Life Science Co., Ltd., Shenzhen, China). The catheters were then attached to the skull using 502 glue and dental cement. Finally, the incised skin was sutured. After surgery, rats recovered for about one week before used to proceed with the experiments. Tactile sensory thresholds were monitored during the recovery period to ensure that the thresholds returned back to their pre-operative baseline.

### Tactile sensory testing

Tactile sensory testing was carried out as described previously by Oshinsky et al.<sup>25</sup> Before the actual stimulation, session rats were adapted to the plastic tube restraint for 10 min. Stimulations were administered when the rat was in a sniffing/no locomotion state. A new stimulus was applied only when the rat resumed this position and at least 30 s after the preceding stimulation. Nociceptive thresholds were measured by perpendicularly applying a Von Frey monofilament (North Coast Medical Co., Ltd.) to the periorbital region of the rats

until a positive response was observed. The von Frey stimuli were presented in a sequential descending order to determine the threshold of response. The threshold is defined as a positive response to two of three, or in some cases three of five trials of a single von Frey monofilament. Rats that did not respond to the 10 g stimulus were assigned 10 g as their threshold for analysis.<sup>25</sup> The evaluating experimenter was blind to the experimental group.

### MRI recordings and VBM analysis

After the last infusion of IS or saline, the MRI data were acquired using a 7.0-T Bruker Pharma Scan system (Bruker BioSpin, Ettlingen, Germany) with a 38-mm-diameter birdcage coil. The rats were anesthetized with isoflurane (5% for initial induction and 1.5% during MRI scanning) in a gas mixture of 40% O<sub>2</sub> and 60% N<sub>2</sub>.<sup>26</sup> Respiration rate were monitored throughout the scans. T2-weighted images (T2WI) were obtained using a 2D-RARE sequence with the following parameters: TR = 6200 ms, TE<sub>eff</sub> = 24 ms, flip angle = 180°, FOV = 35 × 35 mm<sup>2</sup>, matrix size = 256 × 256, slice thickness = 0.3 mm, slice gap = 0 mm, total scan time 20 min.

All structural image post-processing was performed by a single, experienced observer who was blinded to

the treatment group. The preprocessing and data analysis were performed using the *spmratIHEP* toolbox for VBM analysis of rat brain images based on the SPM8 software (Wellcome Department of Cognitive Neurology, London, UK), which comprised a set of MRI T2WI rat brain template and corresponding tissue probability maps (TPMs) in Paxinos and Watson space.<sup>27,28</sup> Because of differences between the human and rat brain, the SPM8 processing methods and parameter settings must be modified according to rat brain imaging features. The voxel size of individual brain images was scaled up in the Analyze header by 10 times to better approximate human dimensions, which did not affect interpretation of the statistical results of rat brain.<sup>29</sup> Each rat's original image was spatially normalized based on the customized template and subsequently segmented into gray matter (GM), white matter (WM), and cerebrospinal fluid based on the customized priors. All the segmented images were resliced by  $1.0 \times 1.0 \times 1.0 \text{ mm}^3$  voxels. This procedure yielded "unmodulated" GM and WM images. Then, voxel values in segmented images of GM and WM were multiplied by the Jacobian determinants to preserve within-voxel volumes that may have been altered during non-linear normalization. This procedure yielded "modulated" images, which were used for the group comparison of GM and WM volume (GMV and WMV). Eventually, both the unmodulated and modulated images were smoothed by a Gaussian kernel of  $242 \text{ mm}^3$  full width at half-maximum. Finally, to identify the differences of GMV and WMV between IS groups and corresponding Con groups, two-sample *t*-test was performed. Brain regions with significant volume changes in rats were yielded based on a voxel-level height threshold of  $P < 0.001$  (uncorrected) and a cluster-extent threshold of 100 voxels.<sup>30</sup>

### Statistical analysis

The SPSS (ver. 20.0; IBM Corp., Armonk, NY, USA) for Windows and GraphPad Prism 5 (GraphPad Software Inc., San Diego, CA, USA) software packages were used for the statistical analyses and graph generation, respectively. Levene's test for homogeneity was conducted, and abnormally distributed data were analyzed using the Kruskal–Wallis test to determine differences among the groups. All data are presented as the mean  $\pm$  standard deviation (SD). A repeated-measures analysis of variance was used to compare von Frey thresholds after the data were examined for normality. Two-sample *t*-test was performed to examine the immunohistochemistry (IHC) difference between groups. Least significant difference *T* tests (when the variance was regular) or Dunnett's *T3* tests (when the variance was irregular) were used to compare the differences

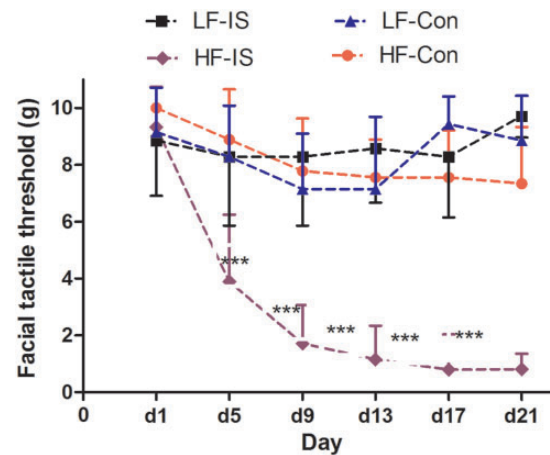


**Figure 2.** Periorbital tactile thresholds during the three-week experiment. Mean  $\pm$  standard deviation values are shown. The horizontal axis shows the time after measurement, and the vertical axis shows the periorbital tactile withdrawal thresholds of the rats. The HF-IS group exhibited significant decreases in periorbital tactile thresholds compared with the HF-Con group (\*\*\*) ( $P < 0.001$ ) from day 5 of the study. No significant differences were shown between the LF-IS and LF-Con groups. HF: high frequency; LF: low frequency; IS: inflammatory soup; Con: control.

between the groups. The level of significance was indicated by  $P < 0.05$ .

## Results

No evidence of brain damage, subdural hematoma, or hemorrhage was detected on T2-weighted images and at the time of euthanasia.

### Changes in the periorbital tactile sensory threshold

The data were abnormally distributed and analyzed using the Kruskal–Wallis test. The facial tactile threshold between LF-IS and LF-Con was not different (Kruskal–Wallis test,  $P > 0.05$ ) (Figure 2). The HF-IS group showed significantly persistent declines in periorbital tactile threshold than those in the HF-Con groups from day 5 (Kruskal–Wallis test,  $\chi^2 = 11.209$ ,  $P = 0.001$ ) (Figure 2). The HF-IS-E and HS-IS-R groups also showed significant declines in periorbital tactile thresholds compared with those observed in the corresponding Con groups from day 5 (Kruskal–Wallis test,  $\chi^2 = 7.084$ ,  $P = 0.008$  and  $\chi^2 = 7.820$ ,  $P = 0.005$ , respectively) (Figure 3). No significant differences in the periorbital tactile thresholds were found between the LF-IS-R and LF-Con-R groups (Kruskal–Wallis test,  $P > 0.05$ ) (Figure 3). These results indicate that only high-frequency infusion of IS led to hyperalgesia and that this state continued to persist after withdrawing the infusion three weeks later.

### Voxel-based morphometry

Significant increases in white matter volume (WMV) were localized in the medulla oblongata and

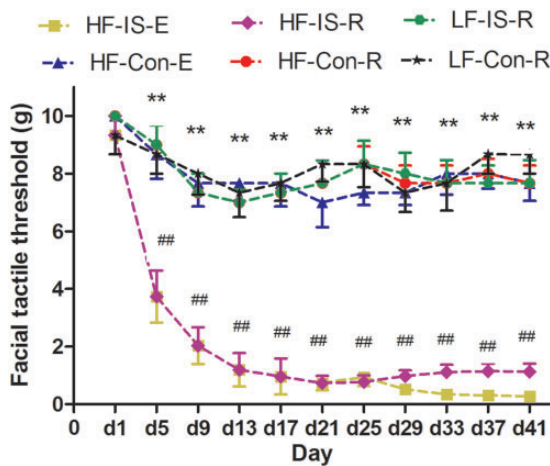


**Figure 3.** Periorbital tactile thresholds during the six-week experiment. Mean  $\pm$  standard deviation values are shown. The horizontal axis shows time after measurement, and the vertical axis shows the periorbital tactile withdrawal thresholds of the rats. The HF-IS-E group exhibited significant decreases in periorbital tactile thresholds compared with the HF-Con-E group (\*\* $P < 0.01$ ) from day 5 of the study. Periorbital tactile thresholds decreased persistently in the HF-IS-R group compared with those in the HF-IS-Con group, even after the IS infusion was stopped (### $P < 0.01$ ). No significant differences were shown between the LF-IS-R and LF-Con-R groups. HF: high frequency; LF: low frequency; E: extension; R: recovery; IS: inflammatory soup; Con: control.

tegmentum of the pons in the LF-IS group compared to the LF-Con group (Figure 4(a) and Table 1) ( $P < 0.001$ , uncorrected, extent threshold  $k = 100$  voxels). Several areas in the HF-IS group showed relative increases in WMV compared to the HF-Con group. These areas included the prefrontal cortex (comprising the cingulate gyrus, anterior cingulate cortex, and medial and prefrontal cortex), the pre-limbic cortex, hippocampus, corpus callosum, and motor cortex (Figure 4(b) and Table 1) ( $P < 0.001$ , uncorrected, extent threshold  $k = 100$  voxels). No significant differences in GMV or WMW were found between the LF-IS-R and LF-Con-R groups. Significant increases in WMV were localized to basal ganglia, corpus callosum, and hippocampus in the HF-IS-R group compared with the HF-Con-R group (Figure 5(a)). The thalamus, periaqueductal gray (PAG), and tegmentum of the pons showed increased GMV in the HF-IS-R group compared with those in the HF-Con-R group (Figure 5(b), Tables 1 and 2) ( $P < 0.001$ , uncorrected, extent threshold  $k = 100$  voxels). The HF-IS-E group showed significantly increased WMV ( $P < 0.001$ , uncorrected, extent threshold  $k = 100$  voxels) in the prefrontal cortex, hippocampus, corpus callosum, and basal ganglia compared with the HF-Con-E group (Figure 6(a)). Areas of decreased GMV included the corpus callosum, basal ganglia, and sensory cortex in the HF-IS-E group compared with the HF-Con-E group, whereas an increase in GMV was detected in the hypothalamus ( $P < 0.001$ , uncorrected, extent threshold  $k = 100$  voxels) (Figure 6(b), Tables 1 and 2).

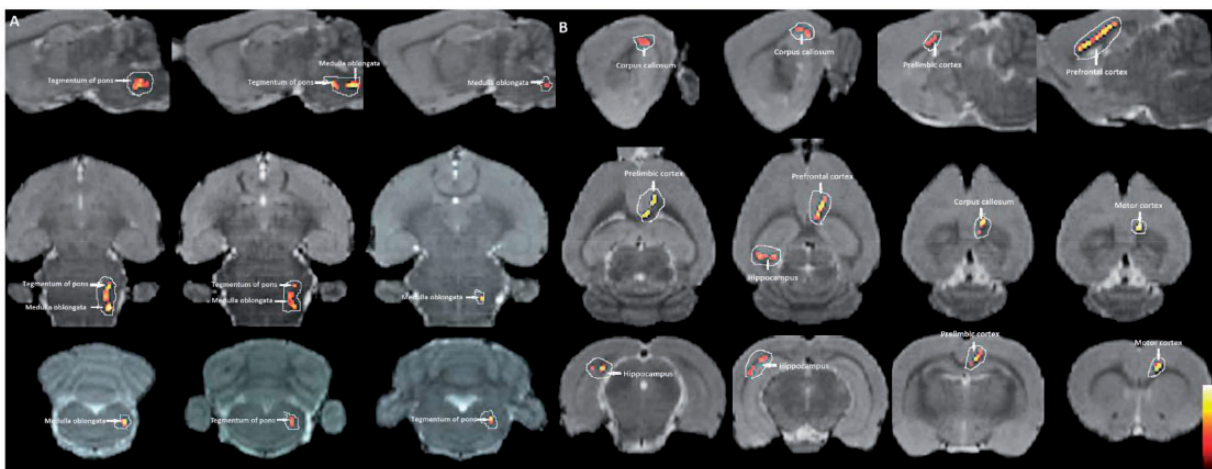


**Figure 4.** Colored voxels represent clusters of significant regional white matter volume increases in the LF-IS group compared with the LF-Con group (a) and the HF-IS group compared with the HF-Con group (b) ( $P < 0.001$ , uncorrected, extent threshold  $k = 100$  voxels) imposed on a T2-weighted magnetic resonance imaging template as well as on the rat atlas structures. Details of the clusters shown are reported in Table 1. HF: high frequency; LF: low frequency; IS: inflammatory soup; Con: control.

**Table 1.** Brain regions with significant WMV changes in rats.

Cluster or region of interest	Coordinates of peak(s) voxel (x, y, z)	Peak <i>T</i> value	Effect direction
Medulla oblongata	2.4, 8.0, -13.3	7.04	LF-IS>LF-Con
Tegmentum of pons	2.3, 7.4, -10.7	5.16	LF-IS>LF-Con
Prefrontal cortex (cingulate gyrus, anterior cingulate cortex, medial prefrontal cortex)	1.2, 2.3, 1.6	8.03	HF-IS>HF-Con
	1.0, 1.7, 1.3	6.78	HF-IS-E>HF-Con-E
Hippocampus	-3.8, 2.4, -6.8	4.53	HF-IS>HF-Con
	2.2, 1.9, -4.9	4.26	HF-IS-R>HF-Con-R
	2.9, 2.2, -5.6	5.10	HF-IS-E>HF-Con-E
Prelimbic cortex	1.2, 2.7, 2.8	3.34	HF-IS>HF-Con
Corpus callosum	1.1, 1.9, -0.8	4.27	HF-IS>HF-Con
	2.3, 1.5, -4.4	4.34	HF-IS-R>HF-Con-R
	2.7, 1.5, -4.7	5.65	HF-IS-E>HF-Con-E
Basal ganglia	1.7, 3.5, 2.2	3.66	HF-IS-R>HF-Con-R
Thalamus	-0.9, 1.8, -1.6	5.19	HF-IS-E>HF-Con-E
Motor cortex	1.2, 1.1, -2.3	6.01	HF-IS>HF-Con

Regions with changes in WMV were found in rats induced by subcranial (supradural) infusion of inflammatory soup compared with saline-treated control rats. The coordinates according to Paxinos and Watson are given in mm x (0 = centre, left is negative), y (ventral to dorsal), and z (relative to bregma). WMV: white matter volume.

## Discussion

The present study examined the time course of recurrent headache-induced structural brain changes in male rats based on the VBM method. We also found the possible structural brain changes associated with periorbital tactile hypersensitivity in IS-infused rats. The key findings of this study are (1) increases in brainstem WMV were observed in the LF-IS group (rat model of EM); areas involved in the processing, modulation, integration, and memory related to pain, including the prefrontal cortex, prelimbic cortex, hippocampus, corpus callosum, and motor cortex showed increases in WMV in the HF-IS group (rat model of CM); (2) as the stimulus time increased, GMV decreased in the corpus callosum, basal ganglia, and sensory cortex, but increased in the hypothalamus of the HF-IS-E group; (3) the brain structural abnormalities in the LF-IS-R group recovered after the stimulation was stopped and the brain structural abnormalities persisted after giving high-frequency IS stimulation, even after the stimulus was stopped; (4) cutaneous allodynia may be associated with structural changes in the pain-integrating and memory areas, including the prefrontal cortex, hippocampus, and corpus callosum.

Despite the large number of human structural imaging studies in patients with migraine showing brain morphological changes related to migraine,<sup>9,31,32</sup> reports of structural imaging in rodent models of migraine are not available. The prevailing view indicates that migraine is abnormal brain functioning that depends on the

activation and sensitization of the trigeminovascular pathway.<sup>33</sup> Existing evidence clearly supports the notion that the brainstem has an important role in the complex pathophysiology of migraine.<sup>34</sup> Consistent with previous MRI studies in patients with migraine,<sup>35–37</sup> structural abnormalities were found in the brainstem (including the medulla oblongata, tegmentum of pons, and PAG) in our study. The LF-IS group showed increased WMV in the medulla oblongata and tegmentum of the pons, suggesting that the brainstem may be involved in the early onset of migraine.

With the increased stimulation of IS (the HF-IS infusion group), brain regions involved in the processing, modulation, integration, affection, and memory related to pain, including the prefrontal cortex, prelimbic cortex, hippocampus, corpus callosum, basal ganglia, thalamus, and motor cortex showed increased WMV. This may indicate the secondary and even third pain processing regions are involved in CM instead of brainstem. WM lesions have been found associated with headache patients in clinics.<sup>38</sup> The WMV changes found in the shorter IS-infused groups in our study indicate that WM is associated with headache and it exists in early stage. Besides similar WMV changes in brain areas with the HF-IS infusion group, a decrease in GMV in the corpus callosum, basal ganglia, and sensory cortex developed with continual dural stimulation (the HF-IS-E group). The decreased GMV changes were consistent with the results of some patients with migraine.<sup>12,39</sup> Clinical researches in migraine showed structural changes in basal ganglia, cingulate cortex, sensory cortex, and so

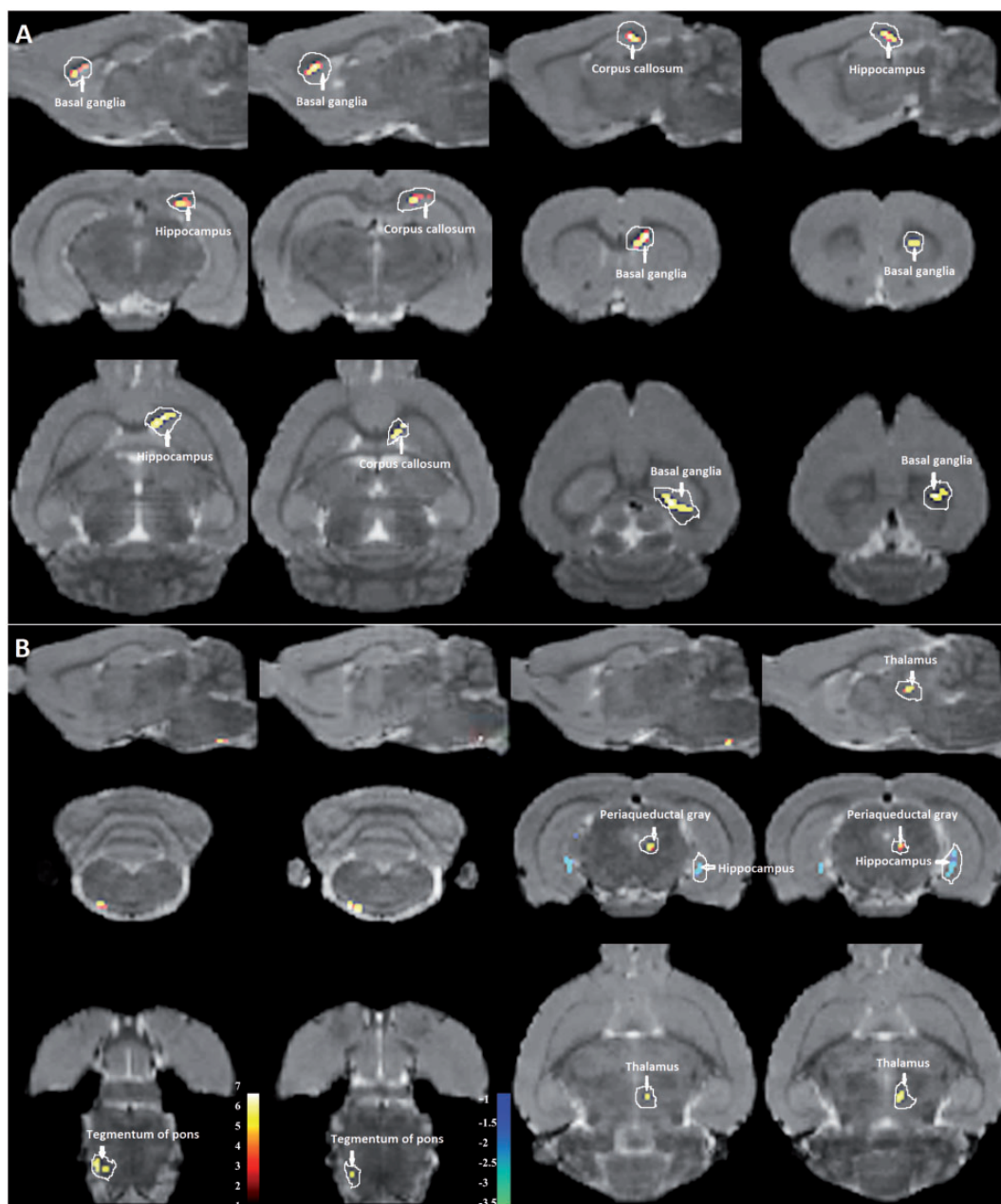


**Figure 5.** Clusters of significant regional white matter volume increases in the HF-IS-R group compared with the HFCon-R group (a) and increased gray matter volume (red) and decreased gray matter volume (blue) (b) imposed on the T2-weighted magnetic resonance imaging template as well as on the rat atlas structures ( $P < 0.001$ , uncorrected, extent threshold  $k = 100$  voxels). Details of the clusters shown are reported in Tables 1 and 2. HF: high frequency; LF: low frequency; IS: inflammatory soup; Con: control.

forth were associated with headache attack.<sup>40,41</sup> The structural brain changes in the HF-IS-E group were associated with repeated stimulation of the meningeal afferents, which indicate that the structural changes in migraine patients may be a consequence of repeated, long-term nociceptive signaling. Moreover, the result further suggested that WM may change prior to GM in pain

condition. Further research can be focused on WM for the interpretation of pain mechanism.

As in previous study, long-lasting cutaneous allodynia did not exist in the LF-IS group after six IS infusions.<sup>24</sup> In the VBM analysis, no supratentorial brain structural changes were shown in the LF-IS group and the brain structural abnormality recovered after

**Table 2.** Brain regions with significant GMV changes in rats.

Cluster or region of interest	Coordinates of peak(s) voxel (x, y, z)	Peak T value	Effect direction
Tegmentum of pons	−1.7, 9.4, −12.6	3.81	HF-IS-R>HF-Con-R
Periaqueductal gray	0.7, 4.9, −6.4	3.62	HF-IS-R>HF-Con-R
Hippocampus	−4.5, 5.7, −5.4	3.98	HF-Con-R>HF-IS-R
Corpus callosum	−5.3, 4.7, −1.1	5.08	HF-Con-E>HF-IS-E
Basal ganglia	−5.1, 4.7, −1.6	4.77	HF-Con-E>HF-IS-E
Thalamus	−2.1, 9.2, −12.4	4.16	HF-IS-R>HF-Con-R
Sensory cortex	−6.4, 3.9, −3.0	5.66	HF-Con-E>HF-IS-E

Areas with GMV changes were found in rats induced by supradural infusion of inflammatory soup compared with saline treated control rats. The coordinates according to Paxinos and Watson are given in mm x (0 = centre, left is negative), y (ventral to dorsal), and z (relative to bregma).

GMV: gray matter volume.

stopping stimulation in the low-frequency IS-infusion rats (LF-IS-R group). Rats received high-frequency infusion of IS showed significant and persisted tactile hyperalgesia even after the stimulation stopped. The corresponding changes between behavior and VBM changes suggested VBM may be used to monitor the progress of migraine. Except the similar WMV changes with the HF-IS infusion group, areas related to pain modulation, including the pons, PAG, and thalamic GMV increased in the HF-IS-R group as observation time increased, even after IS stimulation was stopped. This indicated that the brainstem may be contributed to the generation of migraine. At the same time, the hippocampal GMV declined in the HF-IS-R group compared with HF-Con-R, which is consistent with clinical results in patients with migraine.<sup>42</sup> The behavioral and imaging results in the LF-IS-R and HF-IS-R groups may support the phenomenon that basic headache frequency is associated with migraine progression and reducing migraine attacks in early stage may have the promise of preventing chronicity of migraine or even to reverse it. A longitudinal MRI study performed in the spared nerve injury model reported that increased hyperalgesia is associated with decreased volumes in bilateral S1 hindlimb areas, the anterior cingulate cortex, and the insula.<sup>43</sup> The cutaneous allodynia was existed in the high-frequency IS-stimulation groups, which may be associated with persisted structural changes in the prefrontal cortex, hippocampus, and corpus callosum in those groups. The prefrontal cortex is one of the most prominent areas associated with brain abnormalities in migraine patients, some of them found they were correlated with attack frequency or disease duration.<sup>44</sup> The prefrontal cortex is thought to mediate part of the cognitive dimension of pain processing associated with localization and encoding of the attending stimulus.<sup>45</sup> Previous studies have suggested that the

medial/prefrontal cortex may play a specific role mediating the attenuation of pain perception via cognitive control mechanisms, which are associated with pain modulation.<sup>46</sup> The anterior cingulate cortex is believed to play a critical role in complex cognitive processing, target detection, and response selection and inhibition.<sup>45,47</sup> Numerous studies have provided evidence that the anterior cingulate cortex is engaged in the cognitive-attentional response to pain and the unpleasant emotional experience from pain.<sup>48</sup> Both the hippocampus and corpus callosum play important roles in learning and memory.<sup>49</sup> Previous studies have suggested that pain memory is encoded within the nervous system and that reversing this pain memory may be the key to terminating chronic pain disorders.<sup>50</sup> The results of our study further indicate that cutaneous allodynia is more prevalent in CM especially in interictal phase and may result from structural abnormalities related to cognition, memory, and learning.

Although there are important benefits of using animal models in brain imaging research, particularly in longitudinal MRI studies, there are several shortcomings in pain models, especially migraine-related pain. First, the number of rats in each group was relatively small and a longer time is needed for a better comparison to patients with migraine. However, the supradural IS stimulation is a painful experience and the high-frequency infused rats were irritated during the late phase. Second, although the rats may have shown decreased tactile sensory threshold in the periorbital region, whether they were suffering from headache is unknown. However, the consistent structural brain findings with clinical researches in migraine patients may further underscore the utility of IS-infusion rats as a model of migraine in humans. Finally, only male rats were used in our study, we chose male rats to avoid the possible confounding effects of differences in estrous cycles among the female rats.

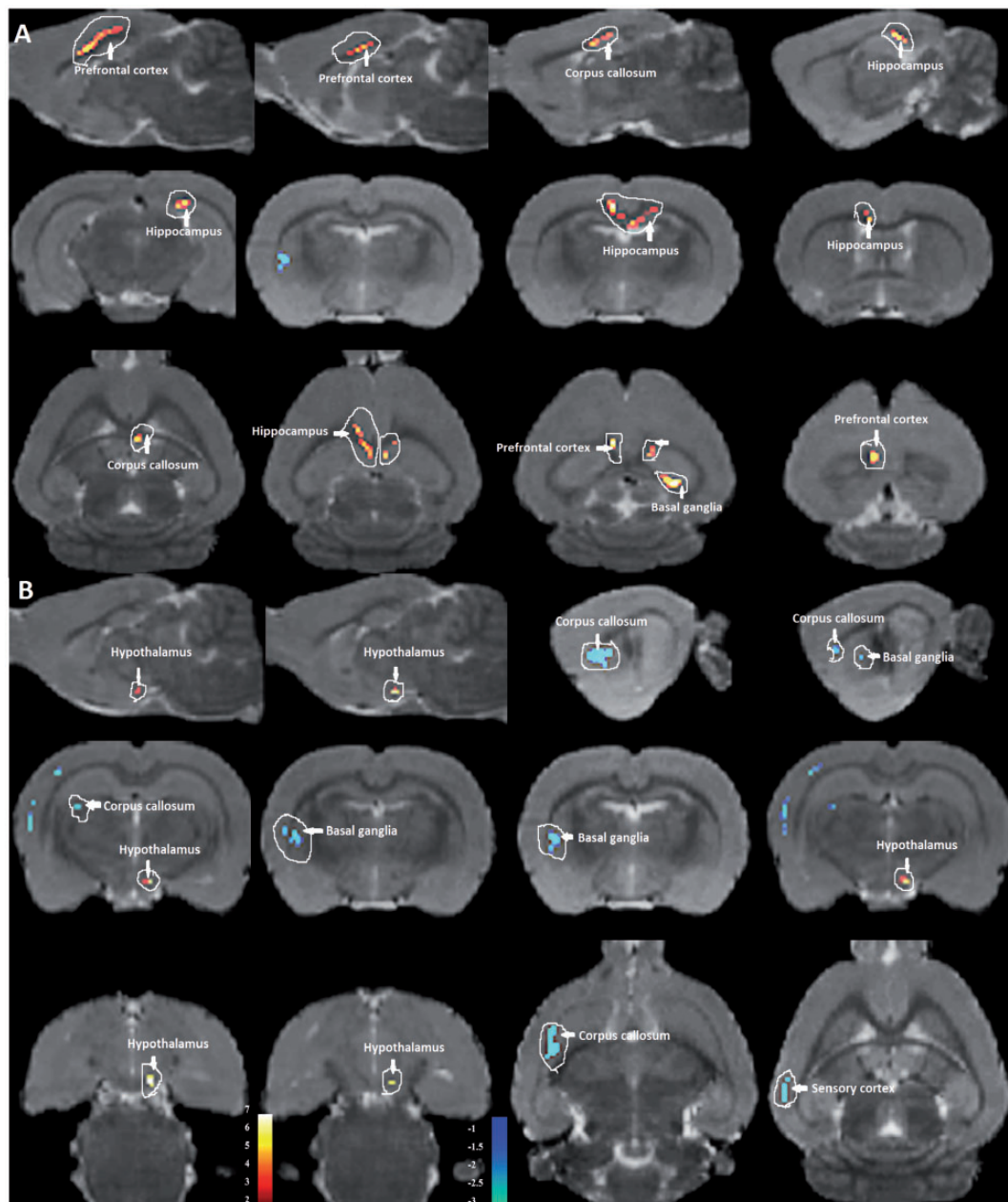


**Figure 6.** Changes in brain volume imposed on the T2-weighted magnetic resonance imaging template as well as on the rat atlas structures in the HF-IS-E rats. (a) Regions of white matter volume are shown; (b) increased gray matter volume (red) and decreased gray matter volume (blue) are shown ( $P < 0.001$ , uncorrected, extent threshold  $k = 100$  voxels). Details of the clusters shown are reported in Tables 1 and 2.

HF: high frequency; LF: low frequency; E: extension; IS: inflammatory soup; Con: control.

Further studies can be performed on female rats to avoid gender bias.

## Conclusion

In summary, longitudinal whole-brain VBM studies demonstrated that a structural abnormality in the brainstem may be involved in early onset of migraine and

contributed to the generation of migraine. The changes of VBM in migraineurs may be a consequence of recurrent headache. VBM can be used to monitor the progress of migraine. The prefrontal cortex, hippocampus, and corpus callosum may be correlated with cutaneous allodynia in interictal phase. Structural changes in brain may be reversed in EM if migraine attack were prevented.

### Author contributions

All authors reviewed the manuscript. Guarantor of integrity of entire study is YSY; WJT and ZHJ designed and supervised experiments; data acquisition and analysis were performed by ZHJ, GQH, and DFZ; RSL raised the mice; manuscript was drafted by ZHJ; manuscript editing was done by YSY; all authors approved the final manuscript.

### Acknowledgments

Authors thank Binbin Nie for the contribution made in the process of VBM data analysis.

### Declaration of conflicting interests

The author(s) declared no potential conflicts of interest with respect to the research, authorship, and/or publication of this article.

### Funding

The author(s) disclosed receipt of the following financial support for the research, authorship, and/or publication of this article: This work was supported by the National Science Foundation of China (grants 81471147, 81500966).

### References

1. GBD 2015 Disease and Injury Incidence and Prevalence Collaborators. Global, regional, and national incidence, prevalence, and years lived with disability for 310 diseases and injuries, 1990–2015: a systematic analysis for the Global Burden of Disease Study 2015. *Lancet (London, England)* 2016; 388: 1545–1602.
2. Dodick D. Clinical practice. Chronic daily headache. *N Engl J Med* 2006; 354: 158–165.
3. Headache Classification Committee of the International Headache Society (IHS). The International Classification of Headache Disorders, 3rd edition (beta version). *Cephalalgia* 2013; 33: 629–808.
4. Aurora SK and Brin MF. Chronic migraine: an update on physiology, imaging, and the mechanism of action of two available pharmacologic therapies. *Headache* 2017; 57: 109–125.
5. Draganski B and May A. Training-induced structural changes in the adult human brain. *Behav Brain Res* 2008; 192: 137–142.
6. Pan PL, Shi HC, Zhong JG, et al. Gray matter atrophy in Parkinson's disease with dementia: evidence from meta-analysis of voxel-based morphometry studies. *Neurol Sci* 2013; 34: 613–619.
7. Sharifi S, Nederveen A, Booij J, et al. Neuroimaging essentials in essential tremor: a systematic review. *Neuroimage Clin* 2014; 5: 217–231.
8. Zhang H, Li L, Wu M, et al. Brain gray matter alterations in first episodes of depression: a meta-analysis of whole-brain studies. *Neurosci Biobehav Rev* 2016; 60: 43–50.
9. Asma Bashir M, Richard B, Lipton M, et al. Migraine and structural changes in the brain. *Neurology* 2013; 81: 1260–1268.
10. Bilgiç B, Kocaman G, Arslan A, et al. Volumetric differences suggest involvement of cerebellum and brainstem in chronic migraine. *Cephalalgia* 2016; 36: 301–308.
11. Jia Z and Yu S. Grey matter alterations in migraine: a systematic review and meta-analysis. *Neuroimage Clin* 2017; 14: 130–140.
12. Liu J, Lan L, Li G, et al. Migraine-related gray matter and white matter changes at a 1-year follow-up evaluation. *J Pain* 2013; 14: 1703–1708.
13. Hu W, Guo J, Chen N, et al. A meta-analysis of voxel-based morphometric studies on migraine. *Int J Clin Exp Med* 2015; 8: 4311–4319.
14. Bigler ED and Maxwell WL. Neuropathology of mild traumatic brain injury: relationship to neuroimaging findings. *Brain Imaging Behav* 2012; 6: 108–136.
15. Seminowicz DA, Laferriere AL, Millecamps M, et al. MRI structural brain changes associated with sensory and emotional function in a rat model of long-term neuropathic pain. *Neuroimage* 2009; 47: 1007–1014.
16. Akerman S, Holland PR and Hoffmann J. Pearls and pitfalls in experimental in vivo models of migraine: dural trigeminovascular nociception. *Cephalalgia* 2013; 33: 577–592.
17. Jia Z, Tang W, Zhao D, et al. Disrupted functional connectivity between the periaqueductal gray and other brain regions in a rat model of recurrent headache. *Sci Rep* 2017; 7: 3960.
18. Melo-Carrillo A and Lopez-Avila A. A chronic animal model of migraine, induced by repeated meningeal nociception, characterized by a behavioral and pharmacological approach. *Cephalalgia* 2013; 33: 1096–1105.
19. Wieseler J, Ellis A, Sprunger D, et al. A novel method for modeling facial allodynia associated with migraine in awake and freely moving rats. *J Neurosci Methods* 2010; 185: 236–245.
20. Mathew NT, Kailasam J and Seifert T. Clinical recognition of allodynia in migraine. *Neurology* 2004; 63: 848–852.
21. Schwedt TJ, Krauss MJ, Frey K, et al. Episodic and chronic migraineurs are hypersensitive to thermal stimuli between migraine attacks. *Cephalalgia* 2011; 31: 6–12.
22. Zimmermann M. Ethical guidelines for investigations of experimental pain in conscious animals. *Pain* 1983; 16: 109–110.
23. Jin C, Yuan K, Zhao L, et al. Structural and functional abnormalities in migraine patients without aura. *NMR Biomed* 2013; 26: 58–64.
24. Oshinsky ML and Gommonchareonsiri S. Episodic dural stimulation in awake rats: a model for recurrent headache. *Headache* 2007; 47: 1026–1036.
25. Oshinsky ML, Sanghvi MM, Maxwell CR, et al. Spontaneous trigeminal allodynia in rats: a model of primary headache. *Headache* 2012; 52: 1336–1349.
26. Sumiyoshi A, Taki Y, Nonaka H, et al. Regional gray matter volume increases following 7 days of voluntary wheel running exercise: a longitudinal VBM study in rats. *Neuroimage* 2014; 98: 82–90.
27. Friston KJ, Holmes AP, Worsley KJ, et al. Statistical parametric maps in functional imaging: a general linear approach. *Hum Brain Mapp* 1995; 2: 189–210.

28. Nie B, Chen K, Zhao S, et al. A rat brain MRI template with digital stereotaxic atlas of fine anatomical delineations in paxinos space and its automated application in voxel-wise analysis. *Hum Brain Mapp* 2013; 34: 1306–1318.
29. Nie B, Liu H, Chen K, et al. A statistical parametric mapping toolbox used for voxel-wise analysis of FDG-PET images of rat brain. *PLoS One* 2014; 9: e108295
30. May A. Pearls and pitfalls: neuroimaging in headache. *Cephalalgia* 2013; 33: 554–565.
31. Maleki N, Linnman C, Brawn J, et al. Her versus his migraine: multiple sex differences in brain function and structure. *Brain* 2012; 135: 2546–2559.
32. Rocca MA, Messina R, Colombo B, et al. Structural brain MRI abnormalities in pediatric patients with migraine. *J Neurol* 2014; 261: 350–357.
33. Pietrobon D and Moskowitz MA. Pathophysiology of migraine. *Annu Rev Physiol* 2013; 75: 365–391.
34. Borsook D and Burstein R. The enigma of the dorsolateral pons as a migraine generator. *Cephalalgia* 2012; 32: 803–812.
35. Chen Z, Chen X, Liu M, et al. Nonspecific periaqueductal gray lesions on T2WI in episodic migraine. *J Headache Pain* 2016; 17: 101
36. Rocca MA, Ceccarelli A, Falini A, et al. Brain gray matter changes in migraine patients with T2-visible lesions: a 3-T MRI study. *Stroke* 2006; 37: 1765–1770.
37. Welch KM, Nagesh V, Aurora SK, et al. Periaqueductal gray matter dysfunction in migraine: cause or the burden of illness? *Headache* 2001; 41: 629–637.
38. Kurth T, Mohamed S, Maillard P, et al. Headache, migraine, and structural brain lesions and function: population based epidemiology of vascular ageing-MRI study. *BMJ (Clinical Research Ed.)* 2011; 342: c7357.
39. Yuan K, Zhao L, Cheng P, et al. Altered structure and resting-state functional connectivity of the basal ganglia in migraine patients without aura. *J Pain* 2013; 14: 836–844.
40. Kim JH, Suh SI, Seol HY, et al. Regional grey matter changes in patients with migraine: a voxel-based morphometry study. *Cephalalgia* 2008; 28: 598–604.
41. Schmitz N, Admiraal-Behloul F, Arkink EB, et al. Attack frequency and disease duration as indicators for brain damage in migraine. *Headache* 2008; 48: 1044–1055.
42. Maleki N, Becerra L, Brawn J, et al. Common hippocampal structural and functional changes in migraine. *Brain Struct Funct* 2013; 218: 903–912.
43. Hubbard CS, Khan SA, Xu S, et al. Behavioral, metabolic and functional brain changes in a rat model of chronic neuropathic pain: a longitudinal MRI study. *NeuroImage* 2015; 107: 333–344.
44. Schwedt TJ and Dodick DW. Advanced neuroimaging of migraine. *Lancet Neurol* 2009; 8: 560–568.
45. Peyron R, Laurent B and Garcia-Larrea L. Functional imaging of brain responses to pain. A review and meta-analysis (2000). *Neurophysiol Clin* 2000; 30: 263–288.
46. Wiech K, Ploner M and Tracey I. Neurocognitive aspects of pain perception. *Trends Cogn Sci (Regul Ed)* 2008; 12: 306–313.
47. Bush G, Luu P and Posner MI. Cognitive and emotional influences in anterior cingulate cortex. *Trends Cogn Sci (Regul Ed)* 2000; 4: 215–222.
48. Rainville P, Duncan GH, Price DD, et al. Pain affect encoded in human anterior cingulate but not somatosensory cortex. *Science* 1997; 277: 968–971.
49. Zaidel DW. The case for a relationship between human memory, hippocampus and corpus callosum. *Biol Res* 1995; 28: 51–57.
50. Price TJ and Inyang KE. Commonalities between pain and memory mechanisms and their meaning for understanding chronic pain. *Prog Mol Biol Transl Sci* 2015; 131: 409–434.